ATMACA Green Route Operations (GRO) Application Report

Deliverable ID:	**D4.1**
Project Acronym:	**ATMACA**
Grant:	**101167070**
Call:	**HORIZON-SESAR-2023-DES-ER-02**
Topic:	**HORIZON-SESAR-2023-DES-ER2-WA2-2**
Consortium Coordinator:	**ESTU**
Edition date:	**12 September 2025**
Edition:	**01.04**
Status:	**Final**
Classification:	**PU**

Abstract

This report presents the development, use, and validation of the Green Route Operations (GRO) application within the ATMACA project. It highlights the benefits of Wind and Temperature Networking (WTN) for flight trajectory prediction and optimisation. By enabling aircraft to share real-time weather data, GRO significantly enhances the accuracy of Estimated Time of Arrival (ETA), fuel efficiency, and environmental performance. Simulations involving over 8,000 flights show that WTN can reduce wind prediction errors by up to 85% and improve trajectory, with greater benefits observed in higher traffic densities. The results demonstrate a scalable, data-driven approach to more sustainable and efficient air traffic management.

EUROPEAN PARTNERSHIP

Co-funded by the European Union

Authoring & Approval

Author(s) of the document

Organisation name	Date
Supatcha Chaimatanan / ENAC	04/07/2025
Huijuan Yang / ENAC	04/07/2025
Daniel Delahaye / ENAC	04/07/2025

Reviewed by

Organisation name	Date
Raquel Delgado-Aguilera/UPM	24/07/2025
Rosa Maria Arnaldo/UPM	24/07/2025
Guillermo Martin/UPM	24/07/2025
Raouf Hamzaoui/DMU	24/07/2025
Hassna Louadah/DMU	24/07/2025
Enes ÖZÇELİK/ESTU	24/07/2025

Approved for submission to the SESAR 3 JU by[1]

Organisation name	Date
Fulya Aybek Çetek / ESTU	12/09/2025
Stefano Bonelli and Tommaso Vendruscolo / DBL	12/09/2025
Raouf Hamzaoui / DMU	12/09/2025
Georges Mykoniatis / ENAC	12/09/2025
Ángel Carmona / SAERCO	12/09/2025
Sergun Özmen / THY	12/09/2025
Rosa María Arnaldo / UPM	12/09/2025

[1] Representatives of all the beneficiaries involved in the project

Rejected by[2]

Organisation name	Date

Document History

Edition	Date	Status	Company Author	Justification
01.01	20/06/2025	Initial Draft	ENAC	Initial version
01.02	20/06/2025	Draft	ENAC	Revised after internal review
01.03	07/09/2025	Final Draft	ENAC	Revised after consortium review
01.04	12/09/2025	Final Revised	ENAC	Approval of the Consortium

[2] Representatives of the beneficiaries involved in the project

Copyright Statement

Disclaimer

ATMACA

AIR TRAFFIC MANAGEMENT AND COMMUNICATION OVER ATN/IPS

ATMACA

This document is part of a project that has received funding from the SESAR 3 Joint Undertaking under grant agreement No 101167070 under European Union's Horizon Europe research and innovation programme.

The UK participant (De Montfort University) is supported by UKRI grant number 10121610.

Table of Contents

List of Figures

List of Tables

Co-funded by the European Union

List of Acronyms

Acronym	Name
ADS-B	Automatic Dependent Surveillance-Broadcast
ADC	Air Data Computer
ATC	Air Traffic Control
ATMACA	Air Traffic Management and Communication over ATN/IPS
ATFCM	Air Traffic Flow and Capacity Management
ATN	Aeronautical Telecommunication Network
CDA	Continuous Descent Approach
ETA	Estimated Time of Arrival
EUROCONTROL	European Organisation for the Safety of Air Navigation
FMS	Flight Management System
FL	Flight Level
GRO	Green Route Operation
IPS	Internet Protocol Suite
LMS	Least Squares Minimization
NWP	Numerical Weather Prediction
OSED	Operational Service and Environment Definition
RTA	Required Time of Arrival
SESAR	Single European Sky ATM Research Programme
SJU	SESAR Joint Undertaking (Agency of the European Commission)
SJU Work Programme	The programme that addresses all activities of the SESAR Joint Undertaking Agency
TMA	Terminal Manoeuvring Area
TOD	Top of Descent
VHF	Work Breakdown Structure
WINTEM	Wind and Temperature aviation weather chart
WTN	Wind and Temperature Networking

1. INTRODUCTION

The aviation industry faces increasing pressure to optimize operations in response to rising traffic demand, fuel costs, and environmental regulations. One of the most effective strategies for achieving operational efficiency and reducing emissions is to improve the accuracy of flight trajectory predictions. However, current trajectory prediction methods still rely heavily on pre-departure meteorological forecasts [1], which often become outdated as flights progress, especially in long-haul operations.

To address this challenge, the ATMACA (Air Traffic Management and Communication over ATN/IPS) project proposes a next-generation air traffic management and communication solution for the Aeronautical Telecommunication Network (ATN). Based on the Internet Protocol Suite (IPS), ATMACA supports the transition from legacy ATN/OSI (Open Systems Interconnection) systems to a modern, flexible, and resilient digital infrastructure. By providing this enhanced communication backbone, ATMACA enables real-time data exchange between aircraft and ground systems.

Within this framework, ATMACA introduces the Green Route Operations (GRO) concept, which aims to dynamically enhance flight trajectory accuracy by integrating real-time wind and temperature updates into trajectory prediction and optimization processes. GRO leverages an air-ground data-sharing framework, known as Wind and Temperature Networking (WTN), which enables aircraft to share atmospheric measurements with each other and with air traffic management systems.

This report evaluates the implementation of GRO through WTN and quantifies its benefits in terms of improved trajectory prediction accuracy, fuel efficiency, and environmental impact reduction. It also outlines the technical methodology, simulation framework, and validation results derived from applying GRO on a dataset of over 8,000 flights.

Unless otherwise stated in this document, the execution of the project will be fully compliant with the latest version of the DES Project Handbook available in the Programme Library:

[1] DES Project Handbook, edition 01.00, 11/04/2022

[2] SESAR 3 Multiannual Work Programme 2022-2031

[3] Grant Agreement n. 101167070

[4] European ATM Master Plan (Executive View), edition 2020

[5] DES HE Requirements and Validation / Demonstration Guidelines, edition 03.00, 15/09/2023

[6] DES Performance Framework, edition 00.01.04, 29/06/2023

[7] DES DSD Communication Guidelines for Project, edition 0.03, 23/11/2022

[8] SESAR JU Common Taxonomy Description O1.00, 07/02/2023

1.1 Purpose and scope

This report presents the application of the ATMACA within the GRO framework, focusing on its benefits for trajectory prediction and optimisation. The purpose is to assess how sharing wind and temperature measurements among aircraft can reduce trajectory prediction errors, enhance Estimated Time of Arrival (ETA) accuracy, and support environmentally efficient flight operations.

The scope includes:

- A conceptual overview of WTN.
- The methodology for implementing real-time trajectory corrections.
- Performance evaluations based on large-scale flight simulations.
- Analysis of impact under varying traffic densities and atmospheric conditions.

1.2 Structure of the Document

The document is organised as follows:

- Section 2 provides the technical background context of trajectory prediction challenges and the GRO concept;
- Section 3 presents the Wind-Temperature Networking concept, including data flow, interpolation techniques, and system architecture;
- Section 4 details the simulation methodology and analyses the benefits of GRO on trajectory prediction performance using wind-only and wind-temperature networking;
- Section 5 discusses advanced applications such as trajectory optimization;
- Section 6 concludes the report, summarising key findings, limitations, and directions for future work;
- Annexes provide supplemental data and references used in the report.

2 BACKGROUND

Accurate trajectory management is central to modern Air traffic Management (ATM), particularly as operations transition toward trajectory-based concepts. Predictability is essential not only for maintaining safe separation and sequencing but also for achieving efficiency and environmental goals. Within this context, the Required Time of Arrival (RTA) serves as a contract between the ATM and aircraft to meet a specific 4D trajectory point [2]. Depending on the accuracy required, the Flight Management System (FMS) may work in a closed-loop mode to target the RTA. While this improves timing precision, it can lead to increased fuel consumption and accelerate engine wear. However, if the FMS operates in an open-loop mode, trajectory prediction errors can accumulate over time, resulting in deviations of up to ±15 Nautical Miles (NM) after one hour of flight [3]. These deviations are primarily linked to inaccuracies in wind and temperature forecasts. More details on the effects of uncertainties of wind and temperature forecasts are discussed in Section 2.1

One significant challenge in balancing fuel efficiency and environmental performance as air traffic demand grows is the uncertainties due to the lack of real-time integration of meteorological data into flight trajectory prediction and trajectory planning. Although modern aircraft are capable of collecting in-flight weather data, there is limited capability to dynamically update and optimise flight routes in real time based on continuously changing atmospheric conditions.

To address this gap, the ATMACA project introduces GRO, leveraging an advanced air-ground communication system. Within this framework, aircraft transmit wind and temperature measurements gathered during their flight to the network, making them available to subsequent aircraft traversing the same airspace. By integrating live updates of weather data (wind and temperature) into trajectory prediction and trajectory optimisation, the GRO can significantly reduce trajectory prediction errors by minimising wind and temperature uncertainties, leading to better adherence to planned flight paths and reducing unnecessary fuel burn.

This supports more accurate trajectory predictions and routing decisions, resulting in:

- More precise arrival time estimates enabling a better organisation of traffic in the Terminal Manoeuvring Area (TMA) with a reduction of vectorings and holdings;
- More accurate estimates of aircraft sector entry times enhance Air Traffic Flow Management3 (ATFM) action efficiency;
- Optimised routing decisions, allowing aircraft to fly a more efficient flight path;
- Lower fuel consumption and CO_2 emissions, contributing to aviation sustainability targets.

The benefits of GRO become more pronounced as the number of participating aircraft in operation increases. When multiple aircraft feed real-time weather data to ATMACA's network, the overall uncertainty reduction is greater, enhancing trajectory prediction across all flights. This improvement is particularly crucial in high-density airspace, where precise trajectory adherence is essential.

[3] **Air Traffic Flow Management (ATFM)** is a collaborative process that ensures the air traffic demand is aligned with available airspace and airport capacity, using measures such as departure slot allocation and traffic sequencing to maintain safety and efficiency.

Conversely, in low-traffic scenarios where trajectory accuracy is less critical, the benefits of GRO may be smaller, but the operational need for precise trajectory adjustments is also reduced.

2.1 Wind and Temperature Networking Concept

Accurate meteorological data, especially wind and temperature information, is crucial for modern aircraft navigation and ATM. Traditionally, forecast data from meteorological services such as WINTEM[4] charts has been the primary source. However, such data is inherently delayed, limited in spatial resolution, and updated infrequently.

The WINTEM forecasts are issued in the form of upper-level wind charts by aviation meteorological services. Their key characteristics include:

- Data derived from observations taken 12 hours prior to the chart's valid time;
- Issued every 3 hours with a validity window of ±3 hours (see Figure 1);
- Provided only at fixed flight levels (e.g., FL050, FL100, FL180, etc.) with limited granularity (see Table 1).

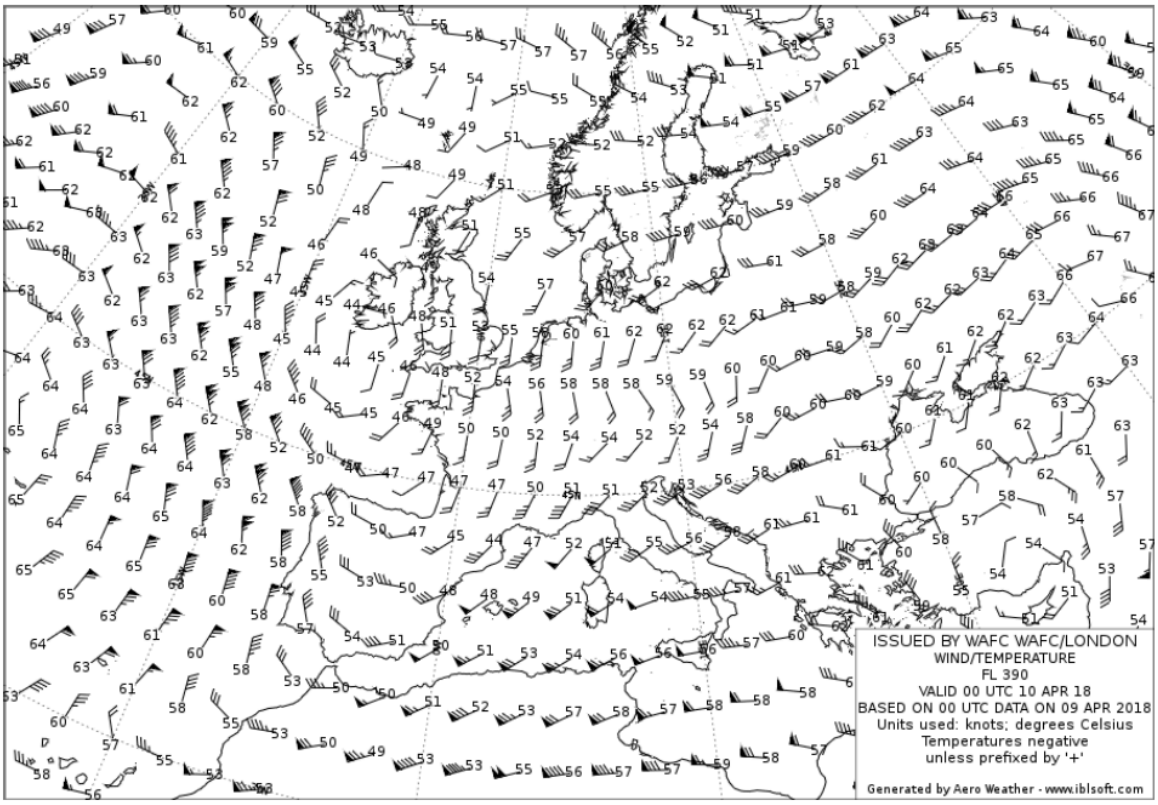

Figure 1 WINTEM data used for forecast and stated valid time

[4] A **WINTEM chart** is an aviation weather chart that provides forecast wind direction, wind speed, and temperature at specific flight levels and times.

FL	20	50	100	140	180	240	270	300	320	340	360	390	410	450	530
Pressure(hPa)	950	850	700	600	500	400	350	300	275	250	225	200	175	150	100

Table 1 WINTEM flight levels availability.

These forecasts work reasonably well for short-haul flights but fall short in several use cases such as:

- Long-haul flights (e.g., >16 hours or 7,600 NM) can extend well beyond the forecast's valid period;
- Rapid atmospheric changes (e.g., jet stream shifts, turbulence zones) cannot be captured in real-time;
- Sparse coverage in uncontrolled or remote airspaces leads to poor vertical and lateral wind profile resolution.

In current operation, the aircraft and air traffic control system rely on predicted wind and temperature data, provided by the meteorological service, to predict aircraft's arrival time to any specific location in the airspace. This Trajectory Prediction (TP) is used for air traffic management, such as aircraft conflict prediction, conflict resolution, sector and TMA entry time estimates, and traffic sequencing. Without timely updates, the lack of accurate wind and temperature inputs can result in:

- Inaccurate fuel burn predictions, leading to contingency fuel usage or diversions;
- Unexpected ATFM reroutings or Flight Level (FL)[5] settings;
- ETAs deviations compromising slot allocations and arrival sequencing;
- Suboptimal cruise altitude selection and inefficient descents.

Practically, this means that if the most favourable route is chosen during the flight preparation based on the predicted wind conditions, it may no longer be the most favourable option three hours after take-off. Without considering wind conditions, any rerouting initiated by the crew will be the great circle between the current position and destination, as it is the shortest ground distance between two points on the Earth's surface. This means that outside trajectory prediction considerations, the update of the wind data has an operational interest. Sharing wind information between aircraft increases the update rate and the number of available wind data samples.

The concept of Wind and Temperature Networking (WTN) is based on modern aircraft's capacity to measure atmospheric data through their Air Data Computers (ADCs). Plenty of accurate temperature and wind data are available in every controlled or uncontrolled airspace. These measurements may be communicated by aircraft to the ground system through the ATMACA protocol. Each time that more recent wind and temperature data are available, the predicted wind and temperature are updated.

With the proposed ATMACA datalink concept, aircraft will be able to exchange such information through the aircraft to the Air Traffic Controller (ATC) datalink. When the atmospheric data derived from the ADS are available, it can be transferred to the ATC or a centralised WTN server. These ground

[5] A Flight Level is a standardized way of expressing aircraft altitude based on an atmospheric pressure setting of 1013.25 hPa,rather than the local air pressure at the surface. It is expressed in hundreds of feet. For example: FL350 = 35,000 ft.

systems then distribute the updated WTN to aircraft whose flight trajectories are predicted to intersect or pass through the same airspace volume.

More precisely, Wind and Temperature Networking is an ATM information-sharing concept that distributes accurate wind and temperature data between ground systems and aircraft via datalink. The WTN provides a robust enhancement to trajectory management by enabling continuous updates of wind data directly to the FMS as more recent observations become available. Unlike traditional methods that rely on static forecasts, WTN incorporates wind measurements encountered by preceding aircraft and applies them across multiple flight levels, not just the current or planned cruise level. This advanced approach leads to more precise fuel consumption estimates after take-off, improved trajectory predictions with greater ETA accuracy, and optimised Top of Descent (TOD) calculations. It also supports environmentally efficient operations such as Continuous Descent Approaches (CDAs), which help reduce fuel burn, emissions, and noise impact on communities during arrival phases. The concept is summarised in Figure 2.

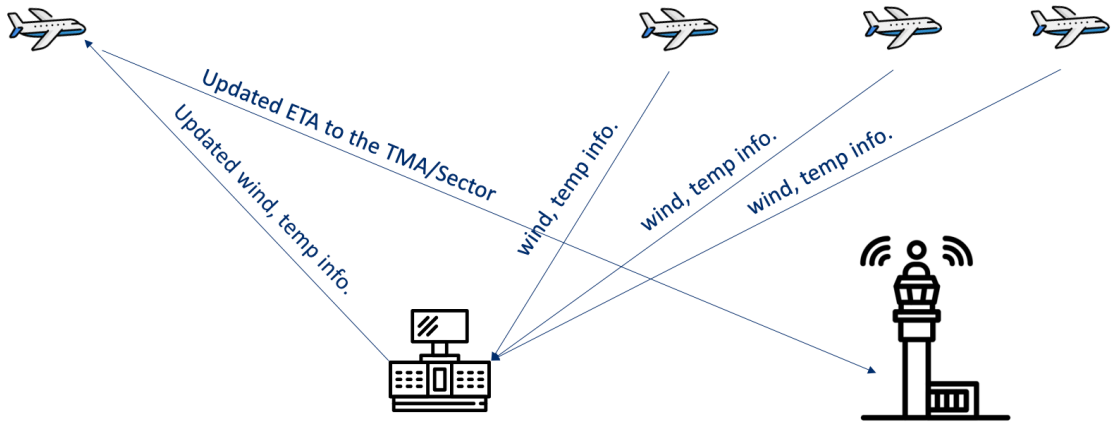

Figure 2 Wind and temperature data network.

3 METHODOLOGY

To construct the wind and temperature map for each flight level, firstly, the airspace is discretized into grids. For each grid, the predicted wind information (wind speed and direction) and temperature obtained from the meteorological service are registered.

In the same manner, the (unknown) true wind and temperature information can be associated with each grid as well. Figure 3 illustrates the discretized wind and temperature grid with predicted and true wind information. (Note: In this figure, only the wind vectors are displayed, while the temperature field is omitted. This choice is made for clarity of visualization.)

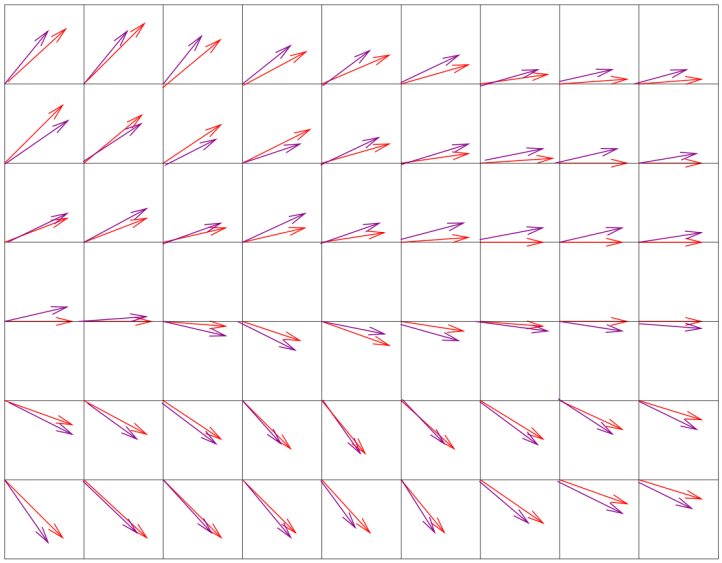

Figure 3 Wind grid with predicted wind information (in red) and true wind information (in purple).

Once the more recent wind and temperature data from the aircraft are available, as illustrated (in blue) in Figure 4, the wind and temperature information are then updated using Shepard's interpolation method [4], which is a widely used technique for estimating values at unknown points based on known data from surrounding points.

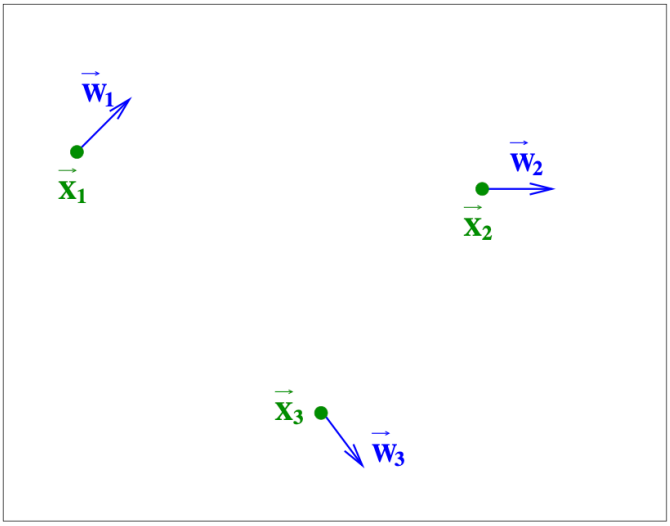

Figure 4 Wind information from aircraft.

Let $F(P)$ be a function of the point $P = (x, y)$ defined for all P in the real plane R^2, the value at point P is the weighted average of the values of N nearby points (grid points of the box where P is located). For the sake of simplicity in explaining the concept, we consider the case with 4 nearby data points P_1, P_2, P_3 and P_4 (integer nodes) as illustrated in Figure 5. Here, "nearby data points" refer to the sample nodes that are spatially closest to the query point P. Their proximity gives them greater influence in the interpolation because the assigned weights are inversely proportional to their distance from P. Denote the value of F at P_i by F_i and let d_i be the distance between P_i and the generic point P in R^2 (See Figure 5). Then F(P) (for this example of 4 nearby data points) is estimated as:

$$F(P) = \left[\sum_{i=1}^{4} F_i \prod_{j\neq i} d_i\right] / \left[\sum_{i=1}^{4} \prod_{j\neq i} d_j\right]. \quad (1)$$

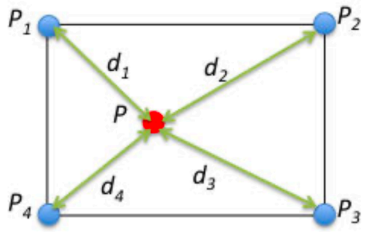

Figure 5 Metric interpolation.

In practice, the nearest data points are chosen from the nodes located within the surrounding grids of P, where the extent of the surrounding grid to be considered may be defined by the user. For N nearby data points, the value of F(P) is estimated as:

$$F(P) = \left[\sum_{i=1}^{N} F_i \prod_{j\neq i} d_i\right] / \left[\sum_{i=1}^{N} \prod_{j\neq i} d_j\right]. \quad (2)$$

Given a set of wind and temperature observations from nearby aircraft (represented by blue arrows in Figure 6), the algorithm constructs a local wind/temperature field over a predefined grid. Figure 6 illustrates the wind field derived from aircraft observations. The temperature field, although included in the model, it is not shown here for clarity of presentation. The next step involves modelling this field using a nonlinear dynamical system, which provides smooth spatial transitions across the grid. The mathematical formulation used to generate this wind/temperature field is based on the following nonlinear system of equations:

$$\vec{W} = \dot{\vec{X}}(t) = \vec{f}(\vec{X}) \quad T = \theta(\vec{X}) \tag{3}$$

where $\vec{X}$ is the state vector of the system $\left(\vec{X} = [x, y, z]^T\right), \vec{f} \in C^2$ be the wind field function that is twice continuously differentiable, and $\theta(\vec{X})$ be the temperature field. These equations associate a vector speed $\dot{\vec{X}}$ and a scalar to a given position in the space coordinate $\vec{X}$.

Based on aircraft observations (positions, wind vectors, and temperature values), the dynamical system is calibrated by minimising the difference between the observed data and the modelled field. This calibration is performed using the Least Squares Minimisation (LMS) method, which determines the model parameters that minimise the squared error between observations and the corresponding predictions, as expressed by the following criteria:

$$E_W = \sum_{i=1}^{i=N} \|\vec{W}_i - \vec{f}(\vec{X}_i)\|^2 \quad E_T = \sum_{i=1}^{i=N} \|T_i - \theta(\vec{X}_i)\|^2 \tag{4}$$

where *N* is the number of observations.

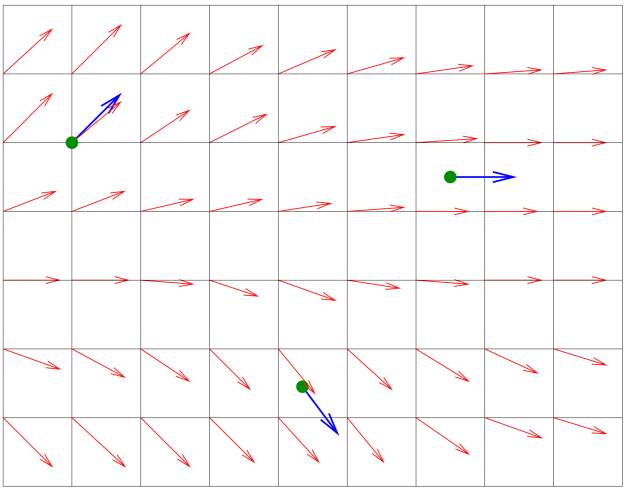

Figure 6 Wind interpolation. The blue arrows correspond to the wind measurements from aircraft. The red arrows represent the Wind field interpolation.

The updated wind and temperature are computed for each cell in the grid, and this updated information can be transmitted to the aircraft and the air traffic controller system. An aircraft receives updates if its planned trajectory passes near the cells previously crossed by other aircraft. The updated information is also provided to the relevant ATC control centres and the flow management system

responsible for the airspace containing those grid cells. This update is not limited to one flight level (e.g., the currently or planned flight level) but provides an update of the predicted winds actually encountered by previous flying aircraft (for more detail, refer to [5]).

4 TRAJECTORY PREDICTION IMPROVEMENT

4.1 Trajectory prediction definition

The problem of aircraft trajectory prediction involves many uncertain factors such as wind, temperature, pressure, aircraft weight, etc. Their influence strongly affects the quality of prediction when the time horizon increases. Let us briefly describe some of them.

- Weight: Aircraft weight mainly depends on the number of passengers, luggage, freight and fuel on board;
- Pilot Actions: Such actions are taken to follow the flight plan, to avoid adverse weather conditions or when controllers change the flight path for conflict resolution purpose.
- Wind: Wind is the major factor impacting trajectory prediction, as it has a direct influence on the ground speed. Furthermore, wind uncertainty is spread in time and in space.
- Temperature: Air temperature is linked to air density (ρ) which drives: aircraft lift $\mathrm{L} = \frac{1}{2} c_L \rho S V^2$ and aircraft drag $\mathrm{D} = \frac{1}{2} c_D \rho S V^2$, where S is the wing surface, V is the aircraft air speed, c_L is the coefficient of lift (ratio of the lift pressure to the dynamic pressure), and c_D the coefficient of drag (ratio of the drag pressure to the dynamic pressure). In addition, it is also linked to True Air Speed (TAS): TAS = aM = $\sqrt{\gamma R T_s M}$, where a is the speed of sound, M is the Mach number, γ is the specific gas ratio constant, R is the air specific gas constant (287.05287 J/(K.kg)),)) and T_s is the static air temperature in Kelvin. Similar to wind, temperature-related errors propagate across both in time and space.
- Engine thrust limits: At higher temperature conditions (reduced air density), maintaining a given Mach number requires an increase in True Airspeed (TAS). In such conditions, thrust limitations may prevent the crew from sustaining the planned Mach number. This deviation from the planned flight profile directly impacts trajectory prediction.

This section discusses the benefit of the proposed wind and temperature networking concept on Trajectory Prediction (TP) accuracy, not by estimating the wind errors but by continuously updating the wind and the temperature using the wind and temperature data available from the neighbouring aircraft that can be transmitted to the ground using the ATMACA framework.

4.2 Methodology

This section describes the methodology used to construct the wind and temperature networking and its application in TP improvement. The steps are detailed as follows:

Step 1: Wind and temperature grid initialisation.
The process begins with the construction of a 4D grid as illustrated in Figure 7. This grid stores both the true and predicted wind and temperature information at each grid point (spatial-temporal node). The four dimensions correspond to latitude, longitude, altitude (covering different flight levels), and time. For clarity of visualisation, only 2D slice of the grid is shown in the figure, and only the wind information is depicted. Then, each aircraft trajectory sample is inserted in the grid. For every trajectory point, three types of wind and temperature values are stored (see Figure 8):

- True wind, true temperature;
- Predicted wind, predicted temperature;
- Updated wind, updated temperature.

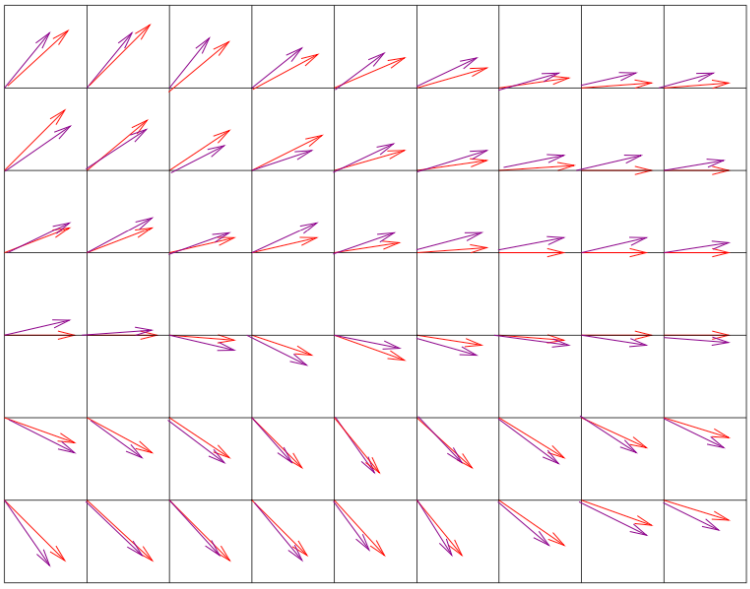

Figure 7 Predicted & True Wind Grid.

Initially, the wind and temperature values are set to the predicted fields. These values are then updated if other aircraft have recently flown through the same or neighbouring grid cells within the last hour. To enable this, each grid cell stores information about aircraft that have passed through it, along with their reported wind and temperature measurements. For each cell corresponding to each trajectory sample, the system checks both the cell and its neighbouring cells for recent aircraft passages and uses the stored measurements to update the predicted values. These updated wind and temperature will be used for the trajectory prediction.

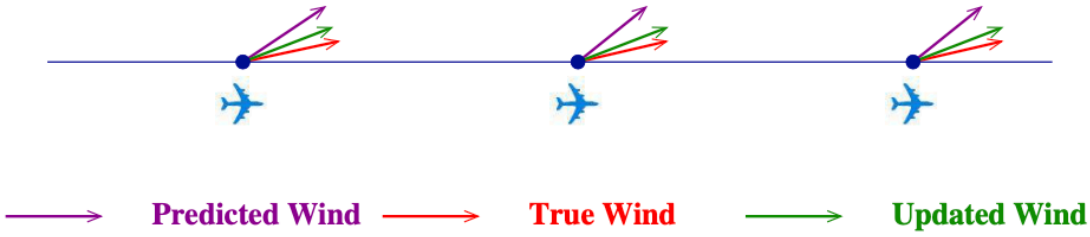

Figure 8 True wind, Predicted wind, and Updated wind associated with each trajectory sample.

Step 2: Efficient neighbour detection in 4D space.

To efficiently identify neighbouring aircraft for wind updates, the same 4D spatial-temporal grid introduced in Step 1 is used. Rather than brute-force pairwise comparisons, aircraft positions are indexed using grid coordinates (latitude, longitude, altitude, and time). Figure 9 shows an example in 2D for clarity: a red dot represents the current aircraft position, and only the immediate surrounding grid cells (red square) are searched for neighbours.

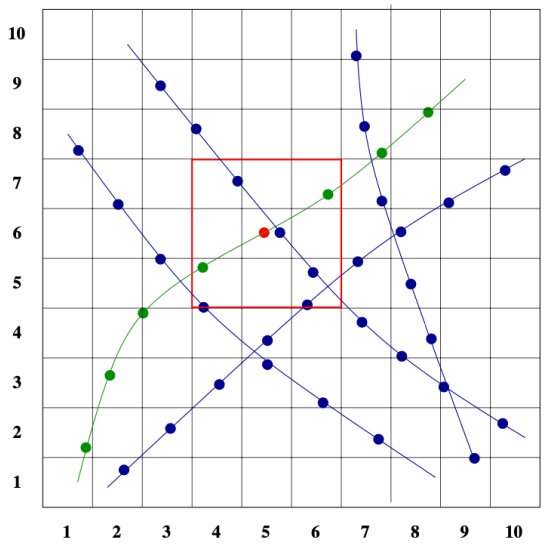

Figure 9 2D slice of the 4D grid used for neighbour detection.

Step 3: Updated wind field computation.

To enhance trajectory prediction, updated wind fields are interpolated based on neighbour aircraft measurements. If a neighbouring aircraft has recorded wind in a nearby 4D cell within the valid time window, the system updates the wind using these more accurate measurements. Then, each trajectory sample has three kinds of wind:

1. Predicted wind;

2. True wind (measured by the aircraft ADC);

3. Updated wind (in case of lack of neighbour, such updated wind is equal to the predicted wind, meaning there is no improvement);

To interpolate sparse measurements, a non-linear dynamical system model is used. Figure 9 shows how the model builds a local wind field using neighbouring aircraft data (blue arrows) and interpolates across a spatial grid (red arrows).

Step 4: Trajectory prediction.

The flowchart in Figure 10 outlines the step-by-step process used to enhance trajectory prediction accuracy through the integration of real-time wind measurements. The method relies on observed aircraft trajectories within a defined spatiotemporal domain and systematically updates ETA calculations using updated wind data derived from neighbouring flights. The key stages of the workflow, shown in Figure 10, are described below:

- Initialization

  Input Data Acquisition: The system begins by reading aircraft trajectory data within a three-dimensional (3D) spatial horizon (latitude, longitude, altitude) and a temporal horizon. These data include flight paths and corresponding timestamps.
- Airspace Structuring

    - 3D Airspace grid building: The observed airspace is limited to the specified spatial horizon and is discretized into 3D boxes (voxels) to facilitate localized wind modelling.
- Wind Data Assignment: Predicted winds (e.g., from GRIB file) and true winds are computed and assigned for each 3D box.
- Wind Assignment to Trajectories
    - Trajectory Wind Mapping: For every trajectory within the spatial domain, the predicted and true wind values are mapped along its waypoints.
    - Pruning Empty Zones: Boxes without any flight paths are excluded to reduce computational load and focus on regions of operational relevance.
- Wind Update
    - Neighbour Trajectory Filtering: For each waypoint, only already flown trajectories are retained as potential sources of updated wind data.
    - Wind Field Interpolation: A wind interpolation algorithm described in Section 3 is applied to construct a continuous wind field across the spatial grid, enhancing resolution and coverage between sparse data points.
- ETA Update and Error Calculation
    - Re-computation of ETAs: Each trajectory's ETA is recalculated using the updated wind values.
    - Error Analysis: The system computes the difference between current and previous ETA estimates at each waypoint. A cumulative error metric is calculated to evaluate overall improvement or deviation.
- Output Generation
    - Final Output: The system outputs updated 4D trajectories (latitude, longitude, altitude, time) with associated ETA errors.

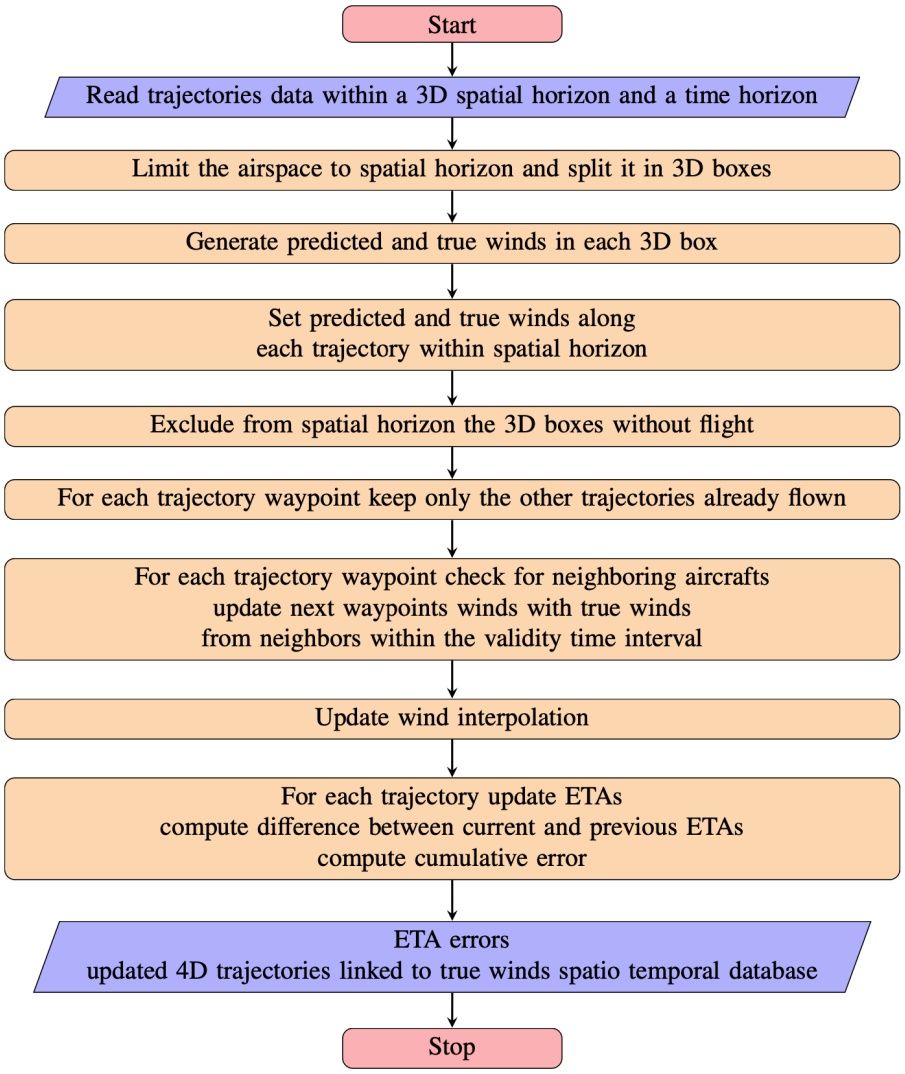

Figure 10 Trajectory prediction block diagram.

4.3 Wind networking

To test the proposed approach, a day of traffic over France for August 12, 2024, which represents the peak summer aviation activity, is considered. For this day, 8,000 flights have been registered. The wind prediction charts are obtained thanks to Meteo France. The first map is considered the predicted wind map (time-stamped *h*), while the second map (time-stamped *h* + 3 hours) is considered the true wind map to simulate real wind.

To test the algorithm, 8,000 flights have been simulated with such winds. Based on the associated flight plans, we first built the aircraft trajectories by using a fast-time simulator (Õirat), a computational tool that reproduces aircraft trajectories efficiently without human interaction, based on the EUROCONTROL Base of Aircraft Data (BADA) database. Such reference trajectories are simulated with the “true wind”. For each trajectory, we compute the trajectory prediction by using the first wind map,

which corresponds to the “predicted wind”. Then, depending on the neighbouring aircraft, the “updated wind” is also computed at each trajectory sample. Based on those three wind values, two performance analyses have been carried out. The first one measures the benefit of the Wind Networking on the wind estimates along trajectories, and the second one measures the associated benefits on the trajectory prediction performance.

4.3.1 Wind prediction error mapping

Figure 11 shows how many trajectories benefited from wind updates based on a sample of 1,000 trajectories. A wind update is considered valid only if the source aircraft passed through the same 4D area less than one hour before the update time. The number of updated trajectories can also be expressed as a percentage, as shown in the figure. The blue curve (left axis) represents the cumulative number of updated trajectories, increasing linearly with the total number of trajectories. The red curve (right axis) shows the percentage of updated trajectories, which rises rapidly and saturates near 100% after only a few hundred trajectories. This indicates that once enough aircraft have flown, almost all subsequent trajectories can benefit from updated wind information, demonstrating the efficiency of the update mechanism.

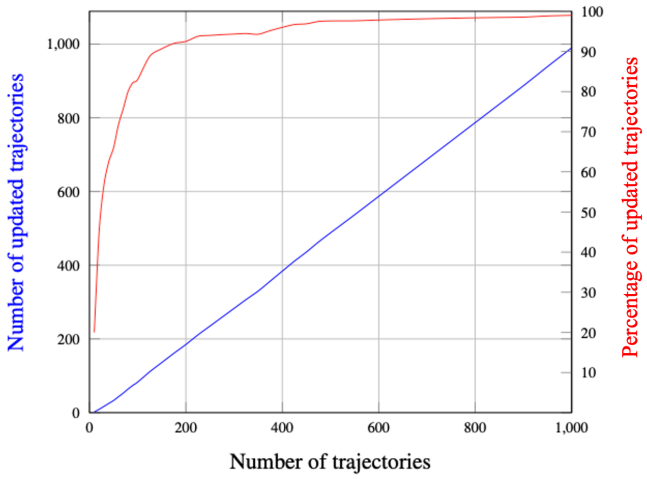

Figure 11 Number of updated trajectories.

Once all three wind types (i.e. true wind, predicted wind, and updated wind) are available along a trajectory, the wind prediction error is calculated as follows:

$$PredWindError = \left| \|PredWind\| - \|TrueWind\| \right|, \quad (5)$$

where ||. || denotes the Euclidean norm (L2 norm) applied to the wind vector. Having computed this error for each trajectory sample, it is possible to build a “Wind Prediction Error map” (see Figure 12) where the wind prediction error on each trajectory sample is represented. The former information is given in three dimensions but is here represented as a 2D graph. The error is computed in terms of norm. The red areas indicate an error of 8 knots. The red dots represent the areas with the biggest errors, and the blue dots those with the smallest errors. The large number of red areas indicates that, without updated information, the predicted wind field deviates substantially from the actual condition encountered by aircraft.

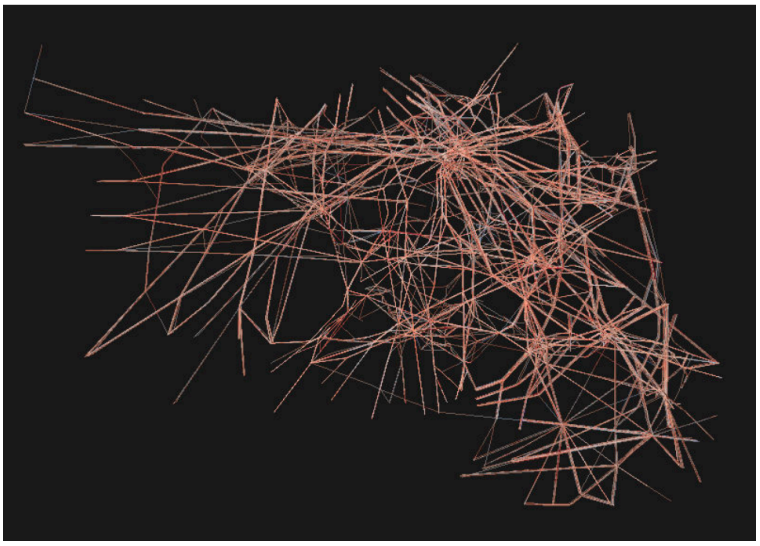

Figure 12 Wind prediction error per trajectory.

This computation has also been done for the updated wind errors:

$$UpdatedWindError = \left| \|UpdatedWind\| - \|TrueWind\| \right|, \quad (6)$$

The associated map is given in Figure 13. We can notice that the red dots have disappeared in high traffic density areas, and that we have much more blue areas, mainly in the high traffic density areas. The aircraft located in low traffic density areas do not benefit from other aircraft data, and do not improve their wind estimates (but their needs for wind updating are less critical as the conflict risk is lower because the traffic spreads out).

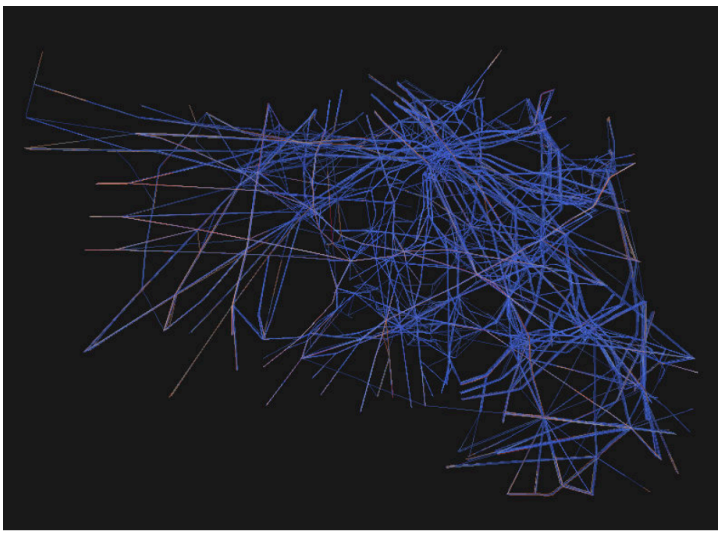

Figure 13 Updated wind error per trajectory.

Finally, we have computed the Wind Networking Improvement by computing the difference between the wind error:

$$Improvement = | PredWindError - UpdatedWindError | \quad (7)$$

This value is positive and is higher when the improvement is also higher. As for the previous values, we can also compute a map for this improvement (see Figure 12). We have just changed the colour representation by setting green colour for large improvement; thus, the green areas indicate where wind networking brings the most improvement (high traffic density areas).

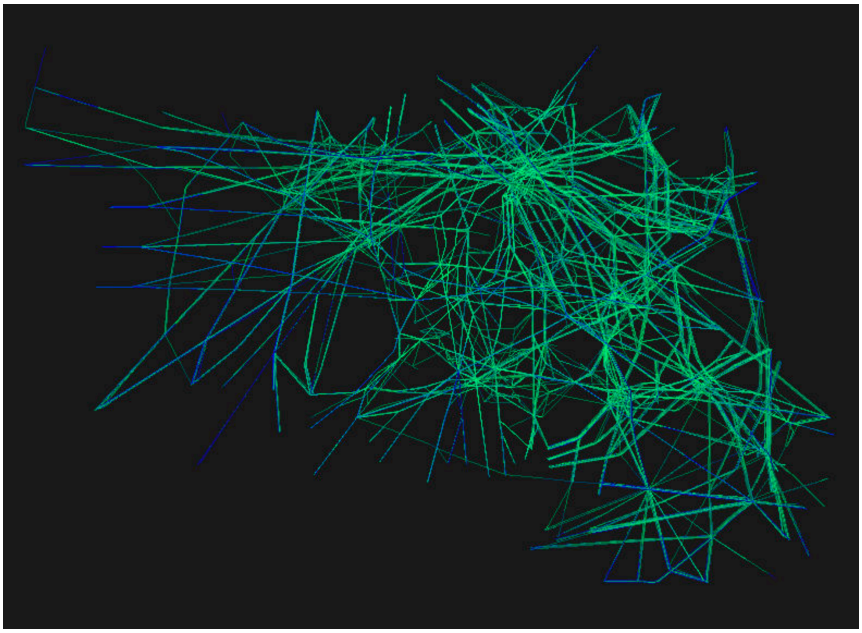

Figure 14 Wind estimated improvement areas.

The second analysis we have performed is linked to the impact of the number of aircraft on the Wind Networking performances. For that, we consider several aircraft densities, and we compute the mean value of each error. Figure 15**Error! Reference source not found.** illustrates the reduction in wind error over the first 1,000 trajectories. The curve shows that most of the improvement from wind networking occurs early. The mean error drops sharply as more trajectories are processed**Error! Reference source not found.** Table 2 extends this analysis up to 8,000 trajectories.

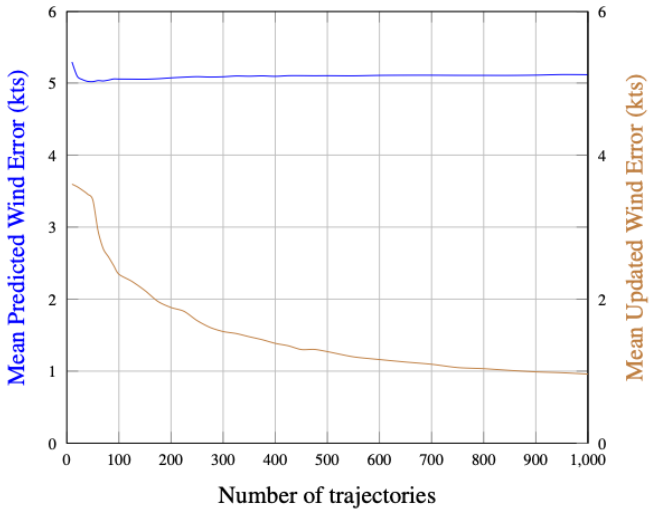

Figure 15 Mean predicted wind and updated wind errors.

Table 2 Predicted & updated wind error.

NbTraj	100	1 000	3 000	5 000	8 000
PredErr (kts)	5.11	5.13	5.12	5.11	5.14
UpdatedErr (kts)	3.23	0.95	0.64	0.5	0.48

For those experiments, we took the first 100 trajectories of the day, then the first 1,000 and so on. With the first 1,000 trajectories, the impact of the Wind Networking is already significant; the wind error drops from 5.13 knots to 0.95 knots, which is 81 % improvement.

4.3.2 Trajectory Prediction Performance

To validate the trajectory prediction performance, we consider that aircraft have to predict their future position at a given horizon all along their trajectory. As shown in Figure 16, at a given location, an aircraft predicts the time it will pass a given point on its future trajectory. Three times have been computed: the *True Time*, the *Predicted Time* and the *Updated Time*. We also compute the following errors:

$$\boldsymbol{PredTimeError} = |\boldsymbol{PredTime} - \boldsymbol{TrueTime}| \quad \textbf{(8)}$$

$$\boldsymbol{UpdatedTimeError} = |\boldsymbol{UpdatedTime} - \boldsymbol{TrueTime}| \quad \textbf{(9)}$$

For different prediction *horizon time (HT)*, we have computed the average Predicted Time Error and the associated Updated Time Error (see Figure 17**Error! Reference source not found.** and Table 3 **Error! Reference source not found.**).

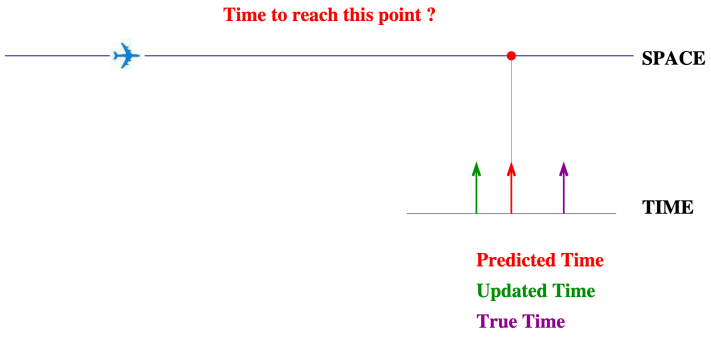

Figure 16 Aircraft position time estimates.

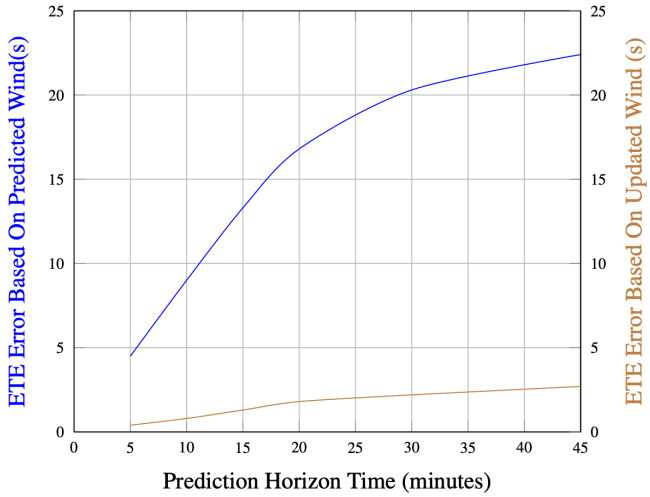

Figure 17 Average Predicted and Updated Time Errors.

Table 3 Predicted & updated time errors.

HT (minutes)	5	10	15	20	30	45
Prepicted Error (sec)	4.5	9	13.3	16.8	20.3	22.4
Updated Error (sec)	0.4	0.8	1.3	1.8	2.2	2.7

The results show that the Predicted Time Error grows rapidly with longer horizons (from 4.5 seconds at 5 minutes to 22.4 seconds at 45 minutes), reflecting the accumulation of wind prediction uncertainty. By contrast, the Updated Time Error remains much smaller (from 0.4 to 2.7 seconds), demonstrating that the use of updated wind and temperature data significantly improves trajectory prediction accuracy.

4.3.3 Estimated Time of Arrival Predictions

Accurate prediction of ETA is crucial for efficient air traffic management, particularly in managing sequencing and runway capacity. Errors in ETA can lead to scheduling conflicts and reduced system efficiency.

To evaluate the impact of Wind Networking on ETA accuracy, we compared three versions of ETA for each trajectory:

- The true ETA;
- The predicted ETA (based on forecast winds);
- The updated ETA (using wind information shared via Wind Networking).

We then analysed the variation between the true ETA and both the predicted and updated ETAs across a range of trajectory samples. Let us denote $\Delta ETA_{true/pred}$ as the difference between the maximum error and the minimum error of ETA when using true wind and predicted wind, and denote $\Delta ETA_{true/up}$ as the difference between the maximum error and the minimum error of ETA when using the true wind and the updated wind, respectively.

As illustrated in Figure 18 Winds impact on ETAs., the spread (i.e., the range between the maximum and minimum errors) in ETA prediction is significantly reduced when using the updated wind data. This indicates that Wind Networking contributes to improving ETA accuracy, helping reduce uncertainty.
To further quantify this improvement, we compared the reduction in ETA error spread between the predicted and updated scenarios ($\Delta ETA_{true/pred} - \Delta ETA_{true/up}$). The results, shown in Figure 19 Reduction of ETA errors. Highlight the clear benefit of integrating real-time wind updates from neighbouring aircraft into trajectory predictions.

Figure 18 Winds impact on ETAs.

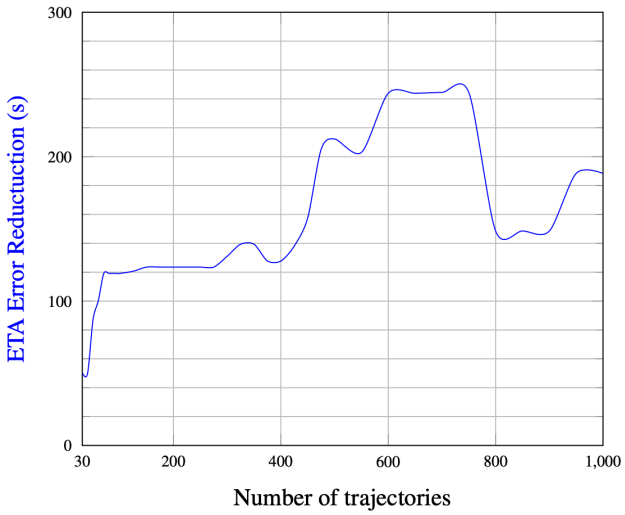

Figure 19 Reduction of ETA errors.

At first glance, the figure suggests a larger benefit with fewer trajectories, since reductions appear stronger early on. This does not mean fewer trajectories are preferable; rather, early predictions are more variable, leaving greater room for improvement. As more trajectories accumulate, overall errors decrease and stabilise, so the relative gain appears smaller, even though ETA accuracy remains consistently better with updated winds.

4.4 Wind and Temperature Networking

Having demonstrated the benefits of Wind Networking alone in improving wind estimation and trajectory prediction accuracy, we now extend the analysis by incorporating temperature data into the networking process. In this section, we assess how the inclusion of shared temperature measurements—alongside wind—further enhances the accuracy of atmospheric modelling and trajectory prediction. This allows us to evaluate the full potential of Wind and Temperature Networking (WTN).

To enhance the computation of updated wind and temperature values, an interpolation algorithm has been implemented. This algorithm uses available measurements from nearby aircraft to construct a local wind/temperature field. The interpolation is based on a nonlinear dynamical system model as described in Section 3, which enables smooth estimation of atmospheric conditions across space. As illustrated in Figure 20, aircraft-provided measurements (blue arrows) are used to populate a 4D grid, on which the interpolated wind and temperature fields are calculated.

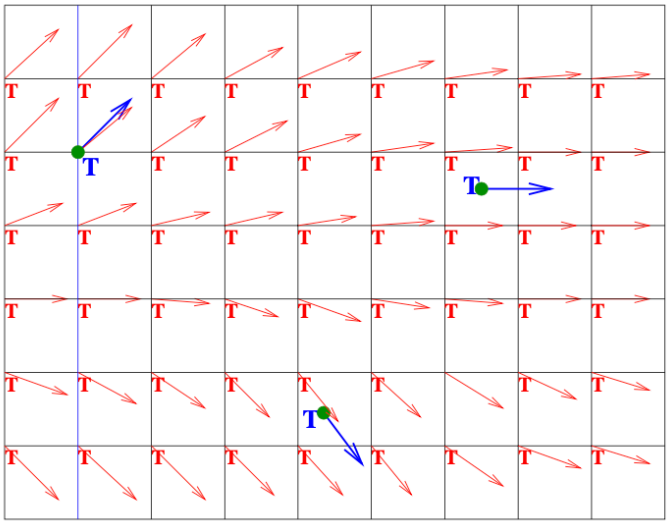

Figure 20 Wind/Temp Field Interpolation

To construct the wind and temperature fields, we apply a nonlinear dynamical system that links each point in space to a wind vector and a temperature value. These relationships are calibrated using aircraft observations—positions, speeds, and temperature—by minimising the fitting error through a least squares approach.

The algorithm proceeds as follows:

1. Generate predicted and actual wind/temperature data in each 4D grid cell;
2. Assign wind/temperature values to each aircraft trajectory;
3. At each trajectory point, identify neighbouring aircraft in space and time;
4. Use their data to refine the local wind/temperature field through interpolation (as detailed in Section 3);
5. Update estimated times of arrival (ETAs) and compare them with predictions.

In the Wind Networking (WN) implementation, the Ground Speed (GS) calculation is refined by adjusting the TAS using temperature corrections (assuming constant Mach number), followed by wind correction. This improves the accuracy of waypoint time estimates and contributes directly to reduce ETA errors.

Temperature variation with altitude was modelled using the ICAO Standard Atmosphere. Aircraft were assumed to fly at constant Mach number, except for turboprops, which can be flagged to apply WN only, excluding temperature corrections.

To validate the WTN concept, we used traffic data from the previous section, covering 8,000 flights. Wind and temperature forecasts from Météo-France (WINTEM maps) at time *h* were used as predictions, while maps at *h + 3 hours* served as the simulated true conditions. Each flight was evaluated under true, predicted, and updated atmospheric conditions. Two key metrics were analysed: improvement in wind/temperature estimation and enhancement in trajectory prediction accuracy through WTN.

4.4.1 Wind/Temp Estimates Performances

For each trajectory sample, three values were recorded: True, Predicted, and Updated wind/temperature. Initially, the updated values match the predicted ones; they are refined using data from neighbouring aircraft when available. These updated values are then used for improved trajectory prediction.

$$PredTempError = | PredTemp - TrueTemp | \quad (10)$$

The second temperature error is linked to the updated and true temperatures:

$$UpdatedTempError = | UpdatedTemp - TrueTemp | \quad (11)$$

Errors related to the wind estimation have already been detailed in section 4.3.

To assess the impact of traffic density on WTN performance, we simulated sets of increasing trajectory counts (100 to 8,000). As shown in Table 4, even with 1,000 aircraft, WTN significantly improves accuracy: wind error drops from 5.13 knots to 0.78 knots, and temperature error drops from 3.01° to 0.45°. These results show that higher aircraft density enhances the effectiveness of WTN.

Table 4 Wind and temperature errors statistics with the number of aircraft.

NbTraj	100	1 000	3 000	5 000	8 000
WindPredErr(knots)	5.11	5.13	5.12	5.11	5.14
WindUpd-Err(knots)	2.30	0.78	0.64	0.5	0.48
TempPredErr(degrees)	3.00	3.01	3.01	3.01	3.01
TempUpd-Err(degrees)	1.45	0.45	0.39	0.38	0.37

4.4.2 Trajectory Prediction Performances

As in section 4.3, in order to validate the trajectory prediction performance, we consider that aircraft have to predict their future position at a given horizon time all along their trajectory

For a given location, three times are computed (the True Time, the Predicted Time and the Updated Time).

We also compute the following errors:

$$PredTimeError = |PredTime - TrueTime| \quad (12)$$

$$UpdatedTimeError = |UpdatedTime - TrueTime| \quad (13)$$

For different prediction *horizon time (HT)*, we have computed the average Predicted Time Error and the associated Updated Time Error.

The first simulation has been done by using Wind Networking only (see Table 5); in this case, we consider that the predicted temperature is the same as the true temperature and only wind prediction

undergoes errors (which is not the case in the real world). As we can see on the table, the impact of the WTN concept is significant for all horizon times.

Table 5 Average time error for different prediction time horizon. (PreDErr shows the average time prediction error without Wind networking, UpdErr show the error with Wind networking.)

HT(minutes)	5	10	15	20	30	45
PreDErr(sec)	4.5	9	13.3	16.8	20.3	22.4
UpdErr (sec)	0.4	0.8	1.3	1.8	2.2	2.7

The same experiment has been done by considering Temp Networking only (see Table 6). In this case, we consider that the predicted wind is the same as the true wind, and only the temperature prediction undergoes errors.

Table 6 Average time error for different prediction time horizons with and without Temp networking.

HT (minutes)	5	10	15	20	30	45
PreDErr (sec)	1.99	3.91	5.78	7.32	9.15	10.34
UpdErr (sec)	0.47	0.97	1.54	2.06	2.70	3.33
% Improvement	76.38	75.19	73.36	71.86	70.49	67.79

Finally, both prediction errors have been included in the simulation, which is the case for the real situations (see Table 7), giving:

Table 7 Average time error for different prediction time horizons with and without Wind/Temp networking.

HT (minutes)	5	10	15	20	30	45
PreDErr (sec)	5.20	10.42	15.68	20.20	25.97	29.00
UpdErr (sec)	0.70	1.41	2.21	3.10	3.83	4.75
% Improvement	86.54	86.47	85.91	84.65	85.25	83.62

Figure 21 compares the percentage improvement in trajectory time error when applying only temperature networking versus combining both wind and temperature networking. The results show that, for all prediction horizons, including both wind and temperature updates provides a consistently higher improvement than temperature-only updates. With temperature networking alone, the improvement remains in the range of 67–76%, while with combined wind and temperature networking it stays above 83%. Although the improvement slightly decreases as the prediction horizon increases (reflecting the accumulation of uncertainty over time), the benefit of Wind Networking remains significant and stable. This highlights that integrating both wind and temperature updates leads to a more robust enhancement of trajectory prediction accuracy across all time horizons. It must be noticed that in the case presented in Table 7, the initial prediction error is the biggest due to the effects of both errors (wind and temperature). The results confirm that applying full WTN significantly improves prediction accuracy across all time horizons.

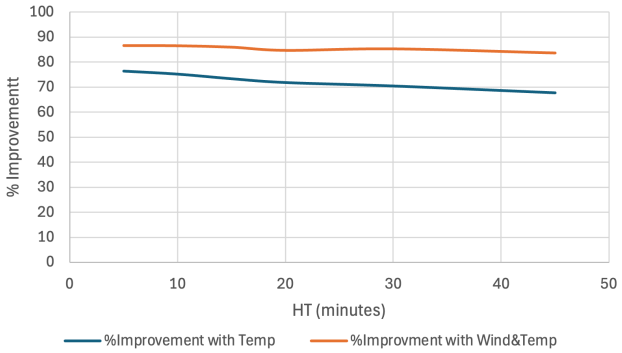

Figure 21 Comparison of improvement using only temperature and both wind and temperature.

4.5 Summary

This section has demonstrated the significant benefits of the proposed Wind and Temperature Networking (WTN) concept on improving aircraft trajectory prediction accuracy. By continuously updating wind and temperature values using data from neighbouring aircraft within a defined 4D spatial-temporal domain, it is possible to substantially reduce prediction errors associated with traditional forecast-based methods.

The algorithm was implemented in Java. The simulation was conducted on an Intel(R) Celeron(R) CPU 847 @ 1.10 GHz, and with 8 GB of RAM. The simulation results, consisting of up to 8,000 trajectories, confirm that WTN enhances both wind/temperature estimation and trajectory prediction performance. Wind prediction errors were reduced from 5.13 knots to 0.78 knots, and temperature errors from 3.01°C to 0.45°C in scenarios involving at least 1,000 aircraft. These improvements directly contribute to more accurate ETA predictions, particularly in high-density traffic areas where the availability of neighbouring aircraft data is higher.

Furthermore, performance comparisons across different prediction horizons indicate that combining wind and temperature networking yields better results than using either input alone. This confirms the operational value of WTN in reducing uncertainty and increasing the robustness of trajectory prediction systems, particularly under the framework of data-driven air traffic management environments such as ATMACA.

5 TRAJECTORY OPTIMIZATION

Wind and temperature conditions are a key source of uncertainty in air traffic operations, as they directly affect an aircraft's ground speed and consequently impact trajectory prediction and arrival time estimation. In particular, variations in wind speed and direction can significantly influence both the current and future positions of an aircraft, presenting a major challenge to accurate and reliable flight planning.

To manage this uncertainty, Numerical Weather Prediction (NWP) centres employ Ensemble Prediction Systems (EPS), which generate multiple weather scenarios by perturbing initial conditions or modifying model parameters. These ensemble members collectively represent a range of possible atmospheric states and are essential for characterising forecast uncertainty. However, despite advances in forecasting techniques, limitations in wind prediction accuracy continue to contribute to scheduling inefficiencies, delays, and airspace congestion, especially in capacity-constrained environments.

Currently, flight routes are typically selected during the pre-departure planning phase based on expected wind conditions. However, due to the inherently dynamic and chaotic nature of the atmosphere, these initially optimal routes can become suboptimal hours into the flight. In the absence of real-time updates, rerouting decisions made enroute often revert to the great-circle path between the aircraft's current position and its destination, disregarding updated meteorological conditions.

A promising advancement in addressing this challenge is the utilisation of in-situ meteorological data collected by aircraft during flight. By sharing this information through Automatic Dependent Surveillance-Broadcast (ADS-B) In/Out systems, aircraft can exchange real-time wind measurements, enhancing situational awareness and trajectory planning across the airspace. This concept, known as WTN, enables downstream aircraft to leverage the atmospheric observations gathered by upstream flights, supporting more informed and adaptive decision-making. This Wind and Temperature Networking concept represents a significant step forward in enabling real-time trajectory optimisation under wind uncertainty.

Building upon the WTN framework, this study proposes a simulation-based optimisation approach that incorporates shared meteorological data into path optimisation at the microscopic level, considering each trajectory segment and local variation in meteorological conditions. Wind uncertainty is modelled using uniform distributions over a graph-based representation of aircraft trajectory, where nodes and links correspond to flight segments. This enables a more granular and realistic modelling of atmospheric variability. The uniform distribution is used as a simplifying assumption to represent wind uncertainty because it allows for a non-biased exploration of possible deviations within a bounded range, without overfitting to a specific probability law. This approach is commonly applied in trajectory simulation studies when detailed probabilistic wind error statistics are unavailable or vary significantly across regions and time horizons. By doing so, we ensure that all potential deviations within the defined bounds are treated with equal likelihood, which provides a conservative and robust basis for testing the Wind Networking concept.

The proposed approach is evaluated using a dataset of over 8,000 flights across French airspace, under diverse traffic and weather conditions. A comparative analysis with standard forecast-based methods is conducted to assess the operational advantages offered by WN. The path optimisation problem is formulated and solved using the Bellman-Ford algorithm, which achieves computationally efficient, high-quality solutions within operational time constraints.

5.1 Wind Initialisation and Link Cost Computation

5.1.1 Wind initialisation

Each node stores 3D positional information in a local coordinate system (ϕ, λ, h), where ϕ, λ and h represent the longitude, latitude and flight level (FL) respectively. For a pair of adjacent nodes, o and d, the displacement vector is computed as follows:

$$\vec{d} = (\boldsymbol{\lambda}_d - \boldsymbol{\lambda}_o, \boldsymbol{\phi}_d - \boldsymbol{\phi}_o) \tag{14}$$

Normalising the displacement vector yields the unit vector $\vec{u}$, which represents the direction of motion between the two points. This unit vector is then used to project wind vectors onto the trajectory direction, enabling the computation of wind components along the path.

$$\vec{\boldsymbol{u}} = \frac{\vec{d}}{|\vec{d}|} = (\boldsymbol{u}_\lambda, \boldsymbol{u}_\phi) \tag{15}$$

Let $\overrightarrow{W_o^m}$ and $\overrightarrow{W_d^m}$ denote the wind vectors at nodes o and d, respectively, with components:

$$\overrightarrow{\boldsymbol{W}_o^m} = (\boldsymbol{W}_{\lambda,o}^m, \boldsymbol{W}_{\phi,o}^m) \tag{16}$$

$$\overrightarrow{\boldsymbol{W}_d^m} = (\boldsymbol{W}_{\lambda,d}^m, \boldsymbol{W}_{\phi,d}^m) \tag{17}$$

for $m \in \{\text{true,pred,updated}\}$

The wind components projected onto the trajectory direction are computed as follows:

$$\boldsymbol{W}_o^m = \vec{\boldsymbol{u}} \cdot \overrightarrow{\boldsymbol{W}_o^m} = \boldsymbol{u}_\lambda \cdot \boldsymbol{W}_{\lambda,o}^m + \boldsymbol{u}_\phi \cdot \boldsymbol{W}_{\phi,o}^m \tag{18}$$

$$\boldsymbol{W}_d^m = \vec{\boldsymbol{u}} \cdot \overrightarrow{\boldsymbol{W}_d^m} = \boldsymbol{u}_\lambda \cdot \boldsymbol{W}_{\lambda,d}^m + \boldsymbol{u}_\phi \cdot \boldsymbol{W}_{\phi,d}^m \tag{19}$$

for $m \in \{\text{true,pred,updated}\}$

Each node connects to multiple neighbours through directional links (see Figure 22), including two northward, two southward, and one eastward link. Direct north-south transitions are intentionally avoided to better reflect real-world traffic patterns in regions such as the North Atlantic Organized Track System (NAT-OTS), where aircraft rarely follow headings of 0° or 180°, even when transitioning between tracks, because the tracks are oriented according to prevailing winds rather than cardinal direction [6].

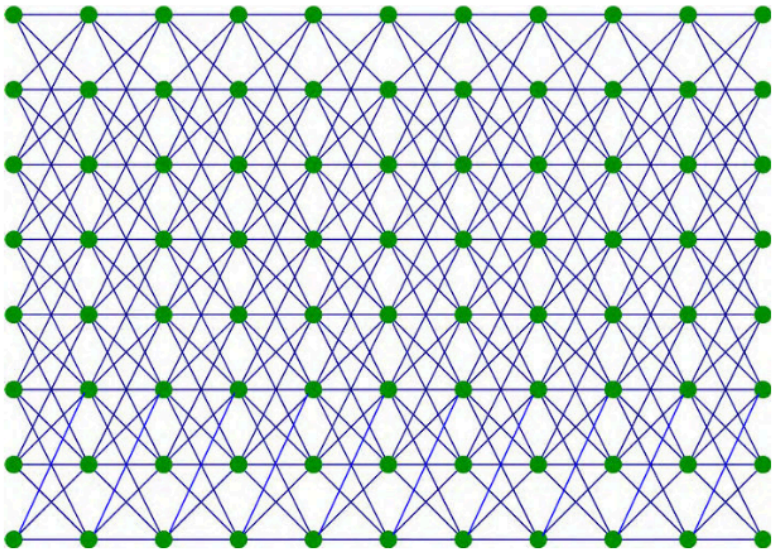

Figure 22 Graph representation for wind-optimal trajectory design.

5.1.2 Link Cost Computation

Let's denote $\mathcal{L}$ as the set of all links in the graph representation of the trajectory design model, for a given link $l = (o, d) \in \mathcal{L}$, connects an origin node o to a destination node d. Nodes correspond to waypoints intersection in the graph representation of the trajectory design model. The average wind component is computed as follows:

$$\overline{W_l^m} = \frac{W_o^m + W_d^m}{2} \quad \text{for } m \in \{\text{true}, \text{pred}, \text{updated}\} \tag{20}$$

The flight time between two nodes depends solely on the air distance, measured in Nautical Air Miles (NAM) and the ground speed, which is determined by the True Airspeed (TAS) adjusted by the wind component along the route. Let V_a denote the TAS, which is assumed to be constant. The resulting ground speed is given by $V_a + \overline{W_l^m}$, and the traversal cost for a link of length D_l is computed as follows:

$$C^m = \frac{D_l}{V_a + \overline{W_l^m}} \quad \text{for } m \in \{\text{true}, \text{pred}, \text{updated}\} \tag{21}$$

5.2 Wind Information Update Mechanism

Each 3D grid cell defined by (ϕ, λ, h) initially assigns its updated wind value to the forecast (predicted) wind. When neighbouring aircraft have recently passed through the region within a specified time window (e.g., one hour), as described in Section 4, the update is performed through interpolation across neighbouring cells to ensure spatial and temporal continuity of the wind field.

This update mechanism is most effective in high-traffic areas, where sufficient neighbouring data is available. In low-density airspace, updates are less frequent but also less critical due to the reduced risk of conflict.

While the updated wind and temperature field improves accuracy, an optimisation step is still required to determine the minimum-cost trajectory. For this purpose, the Bellman–Ford algorithm is adopted. The following section describes the algorithm in detail.

5.3 Bellman-Ford Algorithm

The Bellman-Ford algorithm [7] is a classic shortest path algorithm commonly used in graph theory to determine the minimum-cost path from a source node to all other nodes in a weighted, directed graph.

It is implemented as a resolution algorithm for a prove of concept purpose. Moreover, Bellman–Ford can be implemented in a layered manner, where updates propagate level by level through the graph, which improves computational efficiency by reducing unnecessary relaxations.

Given a graph $G = (N, \mathcal{L})$, where N is the set of nodes and $\mathcal{L}$ is the set of directed links with associated weights w_l, the algorithm has a time complexity of $O(|\mathcal{N}| \cdot |\mathcal{L}|)$.

The algorithm initialises the distance to the source node as zero and sets the distance to all other nodes as infinity. It then iteratively relaxes all edges for $|\mathcal{N}| - 1$ iterations. For each $link\ l = (o, d)$, the following condition is checked:

$$d_o + w_l < d_d$$

where d_o and d_d represent the current shortest known distances from the source to nodes o and d, respectively.

If the condition holds, the distance to node d is updated as follows:

$$d_d = d_o + w_l$$

5.4 Application to Wind-Aware Path Optimisation

In wind-aware flight planning, the Bellman-Ford algorithm is adapted to operate on a grid graph representing a discretised airspace at a fixed flight level. Only aircraft in the cruise phase are considered, assuming constant altitude throughout the optimised segment.

Each node in the grid corresponds to a geographic location, and each directed edge represents a feasible flight segment between neighbouring nodes. The traversal cost for each edge is computed as travel time, which accounts for wind influence through the resulting ground speed.

The path search proceeds from the first column of nodes (entry points) to the last column (exit points), with the Bellman-Ford algorithm identifying the path that minimises the estimated flight time under prevailing wind conditions.

Paths are compared under three wind scenarios:

- True Wind Conditions: computed using actual (ground truth) wind data;
- Predicted Wind Conditions: computed using forecast wind data;
- Updated Wind Conditions: computed using wind data refined by shared measurements from nearby aircraft, as described in the Wind Networking mechanism.

This framework allows dynamic adaptation of planned trajectories in response to real-time meteorological information, improving both prediction accuracy and operational efficiency.

5.5 Case study

5.5.1 Discretised 3D Airspace Description

To model en-route flight operations under varying wind conditions, a structured 3D airspace is constructed, tailored for the cruise phase where aircraft maintain a constant altitude. This discretisation enables efficient wind-aware path computation across spatial and temporal dimensions.

The airspace is represented as a regular 3D grid, with positional data stored in a local coordinate system (ϕ, λ, h). Each grid cell corresponds to a fixed airspace volume, featuring a horizontal resolution of 5 NM in both longitude and latitude directions, and a vertical resolution of 10 FLs per layer, spanning from FL340 to FL380.

To fully enclose all relevant aircraft trajectories, the ϕ axis spans 900 NM from west to east, divided into 180 cells, covering $\phi \in [-520,340]$. Similarly, the λ axis spans 900 NM northwards, covering $\lambda \in [2170,2930]$, also divided into 180 cells. This configuration ensures the grid encompasses all aircraft trajectories of interest within the France area.

5.5.2 Wind Data Simulation and Updating

Figure 23 presents the initial simulated wind fields for both true and predicted winds, overlaid with aircraft trajectories. These wind fields serve as the baseline for the Wind Networking-based update mechanism.

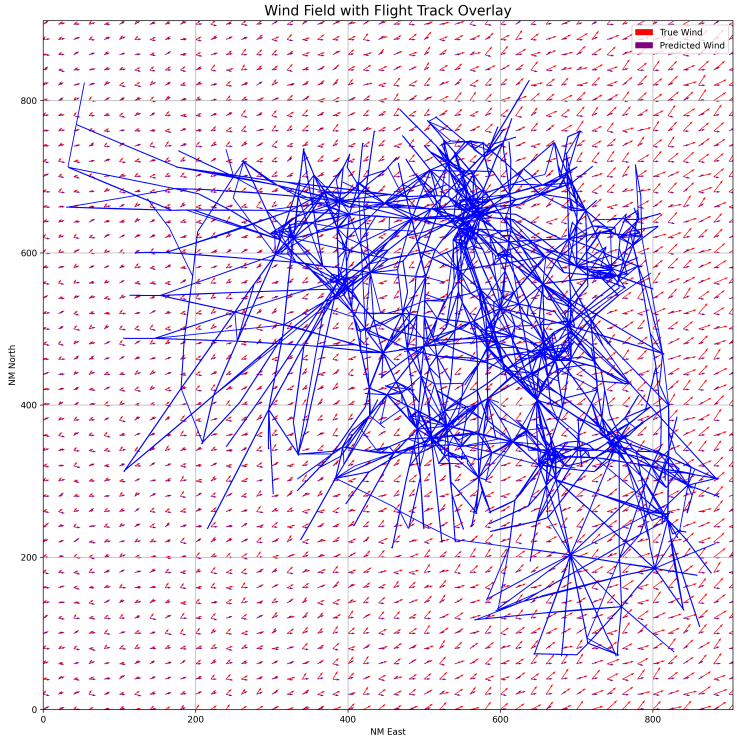

Figure 23 Initial true and predicted wind fields overlaid with aircraft trajectories.

546,127 trajectory points, representing 29.11% of the trajectorie points, fall within the selected 5 FLs. For each trajectory point, the wind data is updated based on a 3D grid. The method iterates over a

5x5x3 window centred around the coordinates of the current trajectory point. This window spans a 5x5 grid in the longitude and latitude dimensions, and a 3-layer window in the FL dimension. Over time, as aircraft traverse grid cells and share in-situ wind measurements, the updated field gradually shifts toward the true wind field, improving alignment with actual atmospheric conditions. This function is essential for synchronising true wind values across adjacent grid points, making it particularly valuable for wind simulations or any system that requires localised updates to wind conditions based on a reference point.

As a result, Figure 24 illustrates the updated wind data at FL360, incorporating aircraft trajectories for FL350, FL360, and FL370. This process ensures that the wind information for neighbouring grid points is aligned with the true wind values of the central point, thereby maintaining consistency across the grid.

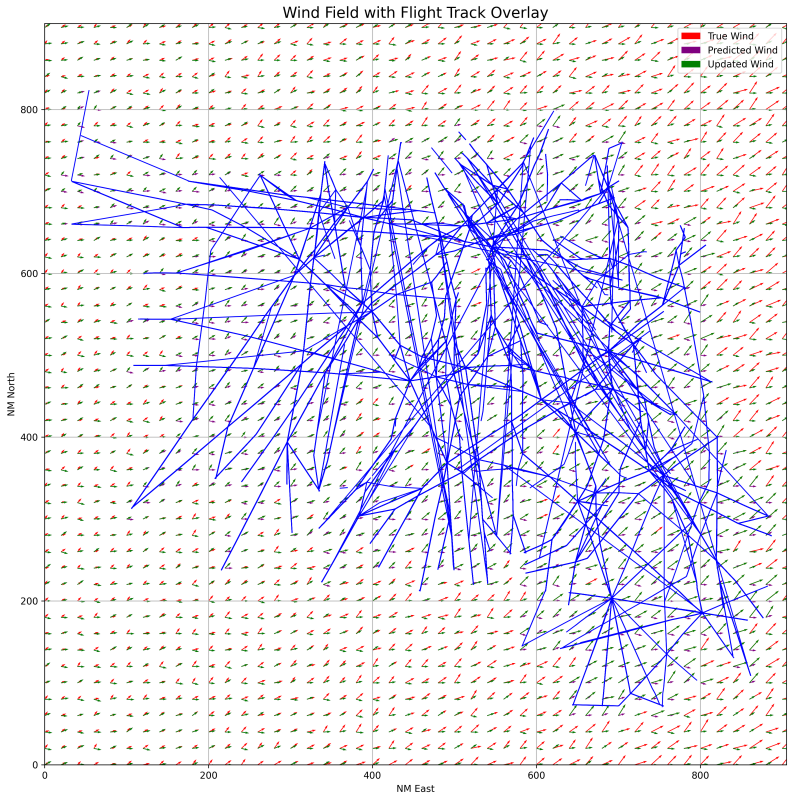

Figure 24 Updated wind field overlaid with aircraft trajectories at FL360.

5.5.3 Traffic Data Filtering and Processing

To validate the proposed wind-aware optimisation framework, we use the same large-scale dataset of 8,000 simulated aircraft trajectories introduced in the previous section. This was generated using the Eurocontrol Base of Aircraft Data (BADA) performance model. The simulation replicates traffic over French airspace on August 12, 2024.

Each trajectory consists of a sequence of time-stamped points containing 3D coordinate information. The FL distribution reveals that most aircraft operate between FL340 and FL380 (see Figure 25), confirming the appropriateness of the vertical extent of the 3D grid.

A spatial filtering step ensures that only points within the defined grid bounds are retained. After filtering, 3,356 trajectories remain, comprising a total of 1,875,818 valid trajectory points.

The filtered traffic dataset is then embedded into a 3D environmental grid, which stores the true, predicted, and updated wind fields at each grid node. These data serve as input to the wind-aware path optimisation module.

A constant TAS of 231.5 m/s (449.9 knots) is assumed for all aircraft during the cruise phase, aligning with typical high-altitude jet cruise speeds.

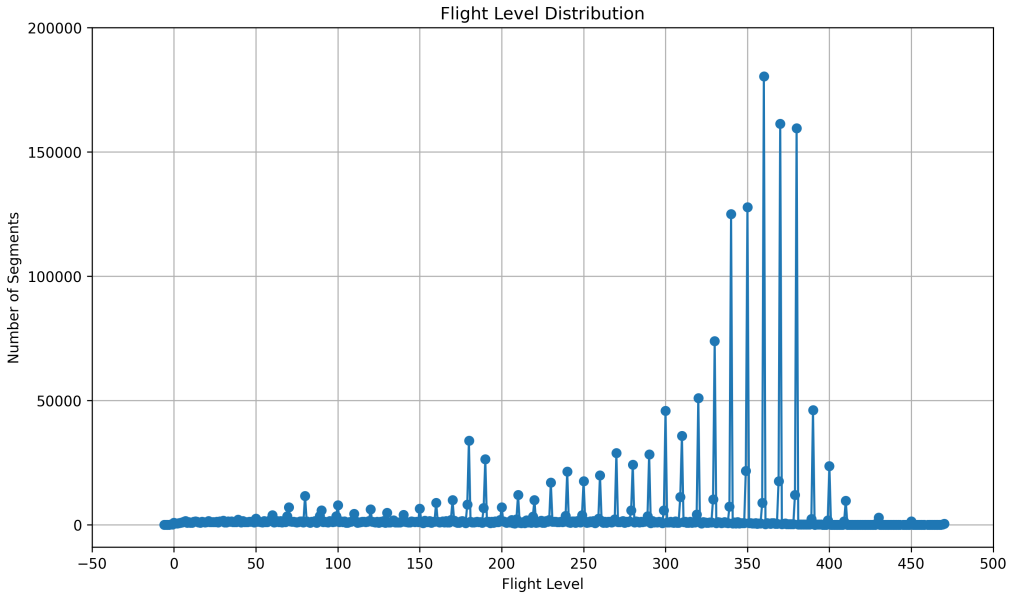

Figure 25 FL distribution of all simulated aircraft trajectories.

5.5.4 Wind-Aware Path Optimisation

The proposed method integrates the Wind Networking concept to enable tailored path optimisation using dynamically updated wind information. A modified Bellman-Ford algorithm serves as the core of the optimisation engine, adapted for a 3D grid-based airspace and multiple wind field scenarios. In this study, the Bellman–Ford algorithm is modified by introducing a layered implementation. Instead of relaxing all edges uniformly in every iteration, updates are propagated level by level across the grid, with only nodes whose costs change being relaxed in subsequent iterations. This reduces unnecessary relaxations and improves computational efficiency.

The simulation was performed using different wind conditions (predicted wind, true wind, and updated wind). On average, the optimisation completes within 10 seconds on a MacBook Air equipped with an 8-core Apple M2 chip and 16 GB of RAM for 1,000 trajectories. The computation comprises two main stages: pathfinding and cost re-evaluation.

- **Pathfinding via dynamic cost propagation.**

In the first stage, pathfinding is performed through dynamic cost propagation based on Bellman-Ford's dynamic programming principle. The cost of the starting node is initialised to zero, while all other nodes are assigned infinite costs. During each iteration, the algorithm scans reachable nodes and

updates their label costs if a cheaper path is identified. This process is executed independently for three wind scenarios, including true, predicted, and updated.

As iterations progress, label costs across the grid are gradually refined. Initially, many nodes retain high-cost values, but as more efficient paths are discovered, these values progressively decrease toward the minimum achievable cost. Each node also records its predecessor to enable reconstruction of the shortest path.

This stage ultimately identifies and stores the shortest path and its associated minimum cost for each wind scenario. Given the iterative nature of the Bellman-Ford algorithm, the cost estimates typically improve over successive iterations.

Figure 26 presents the total costs for each path, calculated using true, predicted, and updated wind data. It highlights the optimality of paths optimised with true wind, as they incur the lowest costs. In contrast, paths optimised with predicted and updated winds exhibit significantly higher costs when evaluated under true wind conditions, reflecting the suboptimality introduced by less accurate wind data.

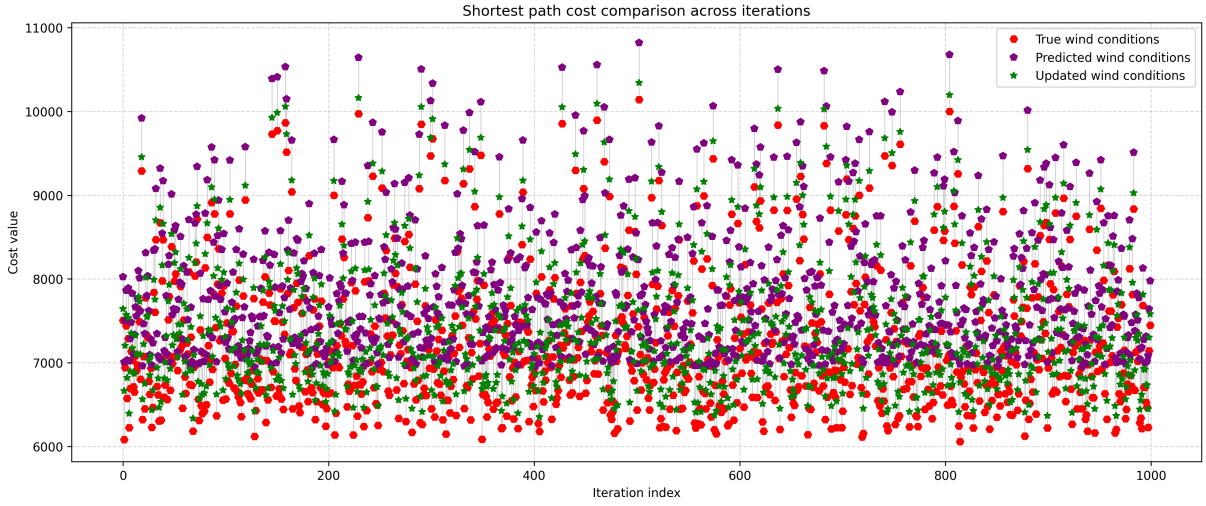

Figure 26 Comparison of minimum path costs across iterations for different wind scenarios.

- **Cost Re-evaluation**

The re-evaluation process offers valuable insights into the effectiveness of path planning under imperfect wind predictions. Specifically, when a path optimised using predicted wind data is re-evaluated with true wind costs, any discrepancy reflects the efficiency loss caused by prediction errors. In other words, only when a path is optimised under true wind conditions does the re-evaluation yield matching costs, validating the accuracy of the optimisation. Conversely, deviations in the re-evaluated costs under predicted and updated wind fields underscore the importance of accurate and synchronised meteorological data.

This approach provides key insights into the accuracy of wind predictions and updates, and their impact on the cost efficiency of optimised flight paths.

- **Computing and Comparing Path Costs**

  This section computes and compares the total costs of paths optimised using true, predicted, and updated wind data. Specifically, it calculates the following:

  1. Total costs for each path optimisation: The algorithm computes the total costs for paths optimised using different wind datasets (true, predicted, and updated).

  2. Extra costs introduced by predicted and updated wind data: The difference in costs between paths optimised with predicted and updated wind data is calculated to evaluate the additional cost introduced by each type of wind data.

  3. Percentage increase in costs due to the use of predicted and updated wind data compared to true wind data:

     This part calculates the difference in total cost between paths optimised using predicted and updated wind data. A positive value indicates that the predicted path is more costly than the updated path, while a negative value suggests that the updated path is more costly than the predicted path. The extra costs with predicted and updated wind data are computed with:

$$\boldsymbol{extraCostPred = (newTotalPredCost - newTotalTrueCost)/newTotalTrueCost * 100} \quad \textbf{(22)}$$

$$\boldsymbol{extraCostUpdated = (newTotalUpdatedCost - newTotalTrueCost)/newTotalTrueCost * 100} \quad \textbf{(23)}$$

     In these formulas, $newTotalPredCost$ and $newTotalUpdatedCost$ denote the cost for paths optimized with predicted and updated wind data, but re-evaluated with true wind. $newTotalTrueCost$ represents the cost for the path optimized with true wind and re-evaluated with true wind. Therefore, those formulas calculate how much more costly the predicted and updated paths are compared to the true wind path, expressed as a percentage.

  4. Difference in Extra Costs between Predicted and Updated Wind-Optimized Paths: Finally, the difference in extra costs between the predicted and updated paths is computed:

$$\boldsymbol{deltaExtraCostPourcent = extraCostPred - extraCostUpdated} \quad \textbf{(24)}$$

     This calculation provides the difference in the percentage of extra costs between the predicted and updated wind paths. The result ($deltaExtraCostPourcent$) reveals whether the predicted wind path is more or less costly than the updated wind path, in terms of percentage differences.

- **Evaluating Performance**

  Lastly, $meanDeltaExtraCost$ and $meanDeltaExtraCostPourcent$ are computed using the following equations:

$$\boldsymbol{meanDeltaExtraCost = meanDeltaExtraCost + deltaExtraCost} \quad \textbf{(25)}$$

$$\boldsymbol{meanDeltaExtraCostPourcent = meanDeltaExtraCostPourcent + deltaExtraCostPourcent} \quad \textbf{(26)}$$

where $meanDeltaExtraCost = 403.3111$ and $meanDeltaExtraCostPourcent = 1.7880\%$. The value of 403.3111 corresponds to an approximate average saving of 6.7167 minutes in flight time. This represents a 1.7880% improvement achieved through the update of wind information, highlighting the effectiveness of the proposed method in reducing costs due to more accurate wind predictions.

5.6 Summary

This section presents a wind-aware path optimisation framework that leverages shared meteorological data to enhance navigation performance in dynamic wind environments. By integrating the Wind Networking concept into a Bellman-Ford-based algorithm, the framework dynamically propagates cost values based on evolving wind conditions, enabling more informed and adaptive route planning.

Three wind scenarios were evaluated: true wind, predicted wind, and updated wind fields incorporating shared meteorological data. The updated wind scenario enabled by collaborative data sharing consistently improves upon the predicted case, demonstrating its value in correcting forecast errors and enhancing real-time trajectory optimisation.

Re-evaluation of the predicted and updated paths using true wind data further reveals the operational impact of forecast uncertainty. The reduced cost discrepancies in the updated scenario demonstrate that shared wind information significantly mitigates uncertainty and improves decision quality.

6 CONCLUSION

As global aviation continues to seek more sustainable solutions, this study confirms that sharing real-time wind and temperature data between aircraft, through WTN, offers a clear path toward more accurate and efficient trajectory prediction and optimisation.

A large-scale simulation, including over 8,000 flights, was performed and demonstrated the tangible benefits of this approach. When only wind updates were considered, significant reductions in wind estimation errors were seen, leading to improved estimation of ETA and prediction accuracy. However, when temperature updates were also introduced, the accuracy improved even further, especially in short- and medium-term trajectory forecasts. This shows that temperature, often underestimated, plays a crucial role in trajectory management, particularly through its impact on true airspeed and ground speed.

When both wind and temperature networking were combined, the system consistently delivered the highest performance, with trajectory time prediction errors reduced by over 85% across all tested horizons. These improvements are not just statistical: they translate into better arrival sequencing, reduced holding, lower fuel burn, and ultimately, fewer emissions. In addition, trajectory optimisation using a modified Bellman–Ford algorithm ensured that the updated atmospheric information could be fully exploited, demonstrating how dynamic cost propagation enables more efficient routing under realistic conditions.

The benefits of WTN scale with traffic density. In busy airspaces, where accurate predictions are critical for maintaining safety and efficiency, the gains from networking become even more pronounced. As each aircraft contributes to a growing, real-time picture of atmospheric conditions, the entire system becomes smarter, creating a collaborative, data-driven foundation for greener and more resilient air traffic operations.

In conclusion, the ATMACA solution, through the GRO framework and its WTN mechanism, offers a practical and effective enhancement to today's trajectory-based operations. It demonstrates how cooperation between airborne systems, supported by modern data links, can reduce uncertainty, improve predictability, and help aviation meet both operational and environmental goals.

This study was based on fast-time simulations and assumed idealised communication and data-sharing between aircraft. Operational constraints such as latency, data-link availability, and integration with controller decision-making were not explicitly modelled. Future work should address these aspects, extend validation to real traffic data, and explore how wind and temperature networking can support concrete ATM strategies such as level changes, vectoring, or delay absorption. Further research should also investigate scalability at the network level and integration into SESAR activities, including OSED and ECO-VAL, to bridge technical findings with operational deployment.

Bibliography

[1] W. Zeng, X. Chu, Z. Su, Y. Liu, and Z. Quan, "Aircraft 4D Trajectory Prediction in Civil Aviation: A Review.," *Aerospace,* vol. 9, no. 2, p. 91, 2022.

[2] EUROCONTROL, Network Management Directorate, "Network 4D Trajectory Concept of Operations (Network 4DT CONOPS)," 4 July 2023. [Online]. Available: https://www.eurocontrol.int/sites/default/files/2023-09/eurocontrol-network-4dt-conops-v1-0.pdf. [Accessed 5 July 2025].

[3] N. E. Dougui, *Planification de trajectoires avion : approche par analogie lumineuse,* Toulouse: Université Paul Sabatier - Toulouse III, 2011.

[4] W. J. Gordon and J.A. Wixom, "Shepard's Method of 'Metric Interpolation' to Bivariate and Multivariate Interpolation.," *Mathematics of Computation,* vol. 32, no. 141, pp. 253-64, 1978.

[5] D. Delahaye and S. Puechmorel, "Air traffic complexity map based on non linear dynamical systems.," in *INO 2005,4th Eurocontrol Innovative Research Workshop & Exhibition*, Paris, France, Dec 2005.

[6] International Civil Aviation Organisation, "Guidance concerning Air Navigation in and above the North Atlantic MNPS Airspace Edition 2011 (NAT Doc 007)," ICAO European and North Atlantic Office., 2011.

[7] R. Bellman, "On a routing problem.," *Quarterly of Applied Mathematics,* vol. 16, no. 1, p. 87090, 1985.